Landscape and Urban Planning 123 (2014) 87–95

Contents lists available at ScienceDirect

Landscape and Urban Planning

journal homepage: www.elsevier.com/locate/landurbplan

Research Paper

Efficiency of parks in mitigating urban heat island effect: An example from Addis Ababa

Gudina Legese Feyisa*, Klaus Dons, Henrik Meilby

Department of Food and Resource Economics, University of Copenhagen, Rolighedsvej 23, DK-1958 Frederiksberg C, Denmark

HIGHLIGHTS

- We evaluated relative cooling effects of urban parks and observed significant cooling differences.
- Cooling effects of green spaces mainly depended on species, canopy cover, size and shape of parks.
- Variation in cooling influence of urban parks was highest in the afternoon hours.
- Appropriate choice of species, geometry and size of parks may improve efficiency of urban warming.

ARTICLE INFO

Article history:
Received 25 May 2013
Received in revised form 6 December 2013
Accepted 13 December 2013
Available online 15 January 2014

Keywords:
Cooling intensity
Cooling distance, Microclimate
Surface temperature
Urban heat island
Vegetation

ABSTRACT

Urban green infrastructure can to a certain extent mitigate urban warming. However, the cooling effect of plants varies with space, time and plant-specific properties. To contribute to our understanding of the cooling effect of vegetation on urban surface and air temperature, 21 parks in Addis Ababa were studied. Air temperature and humidity were measured for 60 plots in nine of the parks for 15 days. Furthermore, the thermal band of Landsat ETM+ was used to examine the cooling impact of all 21 parks on a larger spatial scale. Linear mixed-effects models were used to examine the relationship between characteristics of the vegetation and observed temperature. It emerged that *Eucalyptus* sp. had a significantly higher cooling effect than any other species group ($P < 0.05$) and the species with the least effect on temperature were Grevillea and Cupressus. On a larger spatial scale, the cooling effect of parks on their surroundings (Park Cooling Intensity, PCI) was positively related to the NDVI and area of parks ($P < 0.01$). A negative relationship was observed between PCI and park shape index (SI). The range within which the cooling effect could be observed (Park Cooling Distance, PCD) was positively related to SI and park area. The maximum PCI was 6.72 °C and the maximum PCD was estimated at 240 m. We conclude that the cooling effect is mainly determined by species group, canopy cover, size and shape of parks. Thus, the study provides insights regarding the importance of species choice and spatial design of green spaces in cooling the environment.

Published by Elsevier B.V.

1. Introduction

Urbanization has brought about several undesirable environmental changes. In the process of urbanization, land cover changes and natural surfaces are replaced by the urban fabric which is characterized by higher temperatures than the surrounding rural environment, a pattern described as urban warming. A large body of urban climate studies have shown that thermal, optical and geometric properties of urban surfaces affect heat absorptive and radiative properties and lead to the so-called Urban Heat Island (UHI) effect (Coutts et al., 2007; Gartland, 2008; Krayenhoff & Voogt, 2007; Voogt & Oke, 2003).

High temperatures in urban areas affect health, economy, leisure activities and wellbeing of urban dwellers. In particular, the health of vulnerable people, such as the old and poor, is highly affected by thermal stress caused by warming (Hajat, Kovats, & Lachowycz, 2007; Patz, Campbell-Lendrum, Holloway, & Foley, 2005; Tan et al., 2010). Urban warming may also enhance air pollution, for example by increasing surface ozone concentration with several negative impacts on human health (Jacob & Winner, 2009; Weaver et al., 2009). Furthermore the magnitude and adverse effects of UHI may be intensified as a consequence of global warming (Corburn, 2009). In many tropical countries, where rapid urbanization is undergoing, the intensity and negative impacts of UHI are likely to be substantial (McGregor & Nieuwolt, 1998).

Various strategies are being implemented to improve thermal comfort of outdoor and indoor urban environments. Indoor air conditioning facilities may efficiently eliminate thermal stress. However, this strategy may, at the same time, enhance UHI by

* Corresponding author. Tel.: +45 91414185; fax: +45 353 31508.
E-mail addresses: fgudina@gmail.com, fgudina@life.ku.dk (G.L. Feyisa), kdo@life.ku.dk (K. Dons), heme@life.ku.dk (H. Meilby).

0169-2046/$ – see front matter. Published by Elsevier B.V.
http://dx.doi.org/10.1016/j.landurbplan.2013.12.008

releasing additional heat to the outdoor environment (Tremeac et al., 2012). A study by Shen, Chow, and Darkwa (2013) indicated that in the summer the cooling demand of a typical office building in Hangzhou metropolitan area of China would increase by 10.8% due to ambient temperature increasing by 0.5 °C. Similarly, a study by Akbari, Pomerantz, and Taha (2001) indicated that electricity consumption in US cities on average increases by 2–4% for every 1 °C increase in temperature and estimated that 5–10% of the urban electricity demand is spent on cooling buildings to compensate for 0.5–3.0 °C warming. The increased energy use for cooling may therefore cause other environmental problems such as increased carbon emission. In the context of global climate change, urban buildings are reported to be a major source of greenhouse gas emission (McKibben, 2007). Adaptive strategies of improving thermal environments, therefore, need to aim at lowering energy use in buildings, thereby also reducing carbon emissions (McKibben, 2007; Smith & Levermore, 2008).

Earlier studies have shown that urban green spaces such as parks can considerably mitigate the UHI effect (Georgi & Zafiriadis, 2006; Oliveira, Andrade, & Vaz, 2011; Susca, Gaffin, & Dell'Osso, 2011). The green vegetation can improve both indoor and outdoor thermal comfort, while at the same time providing multiple environmental services, such as carbon storage (Escobedo, Varela, Zhao, Wagner, & Zipperer, 2010; Jana, Biswas, Majumder, Roy, & Mazumdar, 2010; Ren et al., 2011), reduced air pollution (Tallis, Taylor, Sinnett, & Freer-Smith, 2011; Yin et al., 2011) and act as urban biodiversity hotspots (Cornelis & Hermy, 2004). Urban vegetation can also contribute to improving the quality of life and enhancing human well-being through exposure to the nature (Dallimer, Irvine, et al., 2012; Dallimer, Rouquette, et al., 2012). Integration of green spaces in urban planning and building designs may, therefore, be essential for adaptation to and mitigation of thermal impacts of both local and global warming processes.

Different levels of cooling by urban vegetation have been reported in the literature, depending on the methods used and the environments where under which studies are undertaken. Studies that involved ground-based air temperature measurements have shown park cooling effects of 1–7 °C (Chang et al., 2007; Shashua-Bar, Pearlmutter, & Erell, 2009). Studies involving remote sensing techniques where surface temperature data were derived from thermal infrared bands of satellite sensors also reported a large variation in cooling effects of urban green areas (Chen et al., 2012).

According to a review paper by Bowler, Buyung-Ali, Knight, & Pullin (2010), most studies on cooling effects of urban vegetation involved measurements within a single park, and only a limited number of studies have examined the cooling effect of parks on surrounding areas. An obvious factor limiting the application of time synchronized air temperature measurements within and at multiple distances from parks is the high cost of such study designs. Thermal remote sensors may, on the other hand, provide a time-synchronized estimate of surface temperature over entire urban surfaces. Estimation of surface temperature from remote sensors provides essential information regarding the thermal properties of land cover which modifies the air temperature of the lowermost part of the urban atmosphere (Voogt & Oke, 2003).

Recently, studies by Schwarz, Schlink, Franck, and Grossmann (2012) and Chen et al. (2012) showed that ground-based air temperature measurements and surface temperature estimated from thermal sensors are positively and significantly correlated. On the other hand, estimates of the cooling effects of vegetation from surface and air temperature measurements may produce different results. Urban climate studies clearly indicate a need for distinguishing between air temperature and surface temperature due to differences in the nature of the data acquisition and the information content of these data types (Arnfield, 2003; Voogt & Oke, 2003). Urban heat island studies based on surface temperature derived from thermal sensors such as those aboard the Landsat satellites are commonly used for assessing intensity of the surface heat island (SUHI), and for relating surface temperature with urban surface energy fluxes in order to characterize landscape properties, patterns, and processes (Quattrochi & Luvall, 1999). Surface temperature modulates the air temperature of the lowermost layers of urban atmosphere and determines surface radiation and energy exchange (Voogt & Oke, 1998). Analysis of thermal infrared data from satellite sensors offers essential information on thermal variation among vegetated surfaces and built-up and other non-vegetated environments by providing simultaneous observations and a dense grid of data across an entire city.

Complex processes are involved in determining the cooling effect of vegetation on daytime air and surface temperature. The vegetation cools the environment through evaporative cooling, shading effects, and its thermal and optical properties (Dimoudi & Nikolopoulou, 2003; Jonsson, 2004; Oke, 1988; Pearlmutter, Bitan, & Berliner, 1999). Compared to impervious surfaces, which generally have high thermal storage capacity and thermal conductivity, vegetation has low thermal storage and admittance (Oke, 1988; Spronken-Smith & Oke, 1999) and is therefore likely to emit less thermal radiation to the environment. However, the cooling impact of plants on air and surface temperature may vary with environmental factors and plant specific thermal and optical characteristics. Vegetation with highly reflective surfaces (high albedo) may reduce surface temperature by reducing the amount and intensity of thermal radiation which may also lower local and downwind ambient air temperatures because of smaller convective heat fluxes from cooler surfaces (Taha, 1997).

For instance, Oke (1988) indicated that coniferous forests have lower albedo compared to deciduous forests, the probable explanation being that conifers trap more radiation due to the rough leaf and canopy structure. An experimental study by Lin and Lin (2010) also indicated that the cooling efficiency of urban parks is mostly influenced by leaf color and foliage density. Plants growing in dry and hot environments have evolved to absorb less radiation through anatomical and physiological adaptations, thereby influencing the thermal environment in a different way than plants in more humid or colder environments (Oke, 1988). The amount of evaporative cooling and reduction in thermal infrared irradiation emitted from plant leaves likely vary with the evapotranspiration, which, among other things, varies considerably with season, climatic conditions and water availability at the local level (Debruin & Jacobs, 1993). Specific plant species have different adaptations and moisture conservation mechanisms (Pugnaire & Valladares, 2007); hence the thermal impact of different species on the environment is likely to vary.

Despite the contributions of research trying to understand the cooling effects of urban vegetation, generalization from the literature is difficult. In their systematic review of studies on thermal effects of urban green spaces, Bowler et al. (2010) noted that most studies have explored the cooling effects considering only one park. The same review paper also showed that only few studies provided data for sites located at different distances from park boundaries. Identifying the biophysical characteristics of vegetation which determine cooling efficiency may help urban planning to mitigate the UHI effect and improve quality of life in cities. Applying ground-based microclimate measurements and satellite remote sensing, the objectives of the present paper therefore are to: (1) examine the variation of the cooling effect of trees in parks and its relationship with tree species and biophysical site variables, (2) examine the thermal influence of green areas on surrounding environments and identify the main determinants of the thermal contrast and the maximum distance within which cooling can be detected.

2. Methods

2.1. The study area

This study was undertaken in Addis Ababa (9°01′01″ N and 38°45′08″ E), which is the capital and the largest city of Ethiopia (Fig. 1). Addis Ababa is one of the most rapidly expanding cities in the country. According to the Central Statistical Agency of Ethiopia (Central Statistics Agency (CSA, 2012) the total population of Addis Ababa was about 3.041 million in 2012 and the total area of the city was 527 km^2. According to UN-HABITAT (2008), the city was among the fastest growing cities in Africa with an average annual growth rate of 4.1% between 1990 and 2006. The city is located at altitudes ranging from 2025 to 3028 m. The mean annual temperature range is 16–18 °C. Addis Ababa receives an average rainfall of 1255 mm per year. A review of climate records for over one hundred years by Conway, Mould, and Bewket (2004) shows an increase of minimum and maximum air temperatures in Addis Ababa of 0.4 °C/decade and 0.2 °C/decade, respectively.

Twenty one green areas (predominantly covered by tree vegetation and with areas ranging from 0.85 to 22.3 ha) were selected. Some of these green areas are not officially designated as parks. In this study we used the term "park" to mean green areas with dense tree vegetation (canopy cover of at least 60%, estimated by visual inspection of high resolution aerial photographs) and a minimum area of about 1 ha. We apply the FAO definition of trees, i.e. woody perennials with a single main stem. The 21 green areas include official public parks, green spaces around churches, government offices and private parks. Little variation was observed in the areas surrounding the selected parks in terms of density and height of buildings, and the areas were considered representative for Addis Ababa. Fig. 1 shows a map where the 21 green areas are overlaid on a Digital Elevation Model (DEM) background.

2.2. Data collection and analysis

We measured air temperature and humidity 1.5 m above ground using automated data loggers and derived surface temperature from Landsat imagery. The ground-based measurements provided high temporal resolution at microclimate level (Hung, Uchihama, Ochi, & Yasuoka, 2006). By contrast, thermal remote sensing provided a simultaneous view of surface temperature at the scale of the entire city, but thermal remote sensing from satellite sensors such as Landsat does not provide sufficient detail on temporal variations in surface temperature. On the other hand, with ground-based measurement, it is difficult to simultaneously record data at multiple points across a large area. Therefore, by combining the two approaches we attempted to overcome their individual limitations and better understand the cooling effects of urban tree vegetation.

2.2.1. Ground-based park microclimate data collection and park characterization

Nine green areas were sampled for the ground-based measurements. A systematic random sampling technique was used within each of the selected green areas to determine the points (plots) where microclimate measurements should be carried out. Sixty sample plots were selected at intersection points of a 60 by 60 m grid which was laid out randomly within each green area. The sample plots were quadratic with a size of 30 by 30 m.

The coordinates of the sample plots were pre-determined by overlaying the grid on the map of the parks using ArcGIS version 10.0. During the field work, it emerged that some locations were inaccessible and a rule of moving plots 30 m North or South was used.

Within each of the 30 m by 30 m sample plots, the following park characteristics were assessed: dominant species (based on share of canopy cover), canopy cover in percent, crown depth of dominant species (measured in meters), ground cover type, and ground moisture condition. Five groups of species were distinguished based on their dominance within the sample plot. These are *Acacia tortilis*, *Eucalyptus* spp. (including *E. grandis*, *E. camaldulensis* and *E. globulus)*, *Grevillea robusta, Cupressus lusitanica* and *Olea* spp.

At the center of each sample plot in the nine parks, temperature and humidity were measured from 10:00 to 15:59 o'clock local time for 15 consecutive days, October 4–18, 2010. Lascar Temperature–Humidity Loggers (model EL-USB-2-LCD) were used for these measurements. The data logging accuracy and repeatability of the sensors were ±0.5 °C and ±0.1 °C for temperature and ±3% and ±0.1% for relative humidity measurements, respectively. All data loggers were set to record temperature every 30 s. In order to cover all sample plots within a park, the data loggers were moved from one location to the next every 5 min (one data logger per park was used). The loggers were mounted 1.5 m above ground on a tripod stand and kept in wooden boxes which were 30 cm in all dimensions. The boxes allowed free air movement while protecting the loggers against direct solar radiation. Due to the interference of park vegetation with air flow at the low height above ground where temperature and humidity were measured, it was considered too difficult to measure realistic wind speeds. In the analysis we therefore had to assume that wind speed was uniform across all parks and sample plots. The month of October typically constitutes the end of rainy season in Addis Ababa. Hence, it was considered a suitable month to study the cooling effect of tree vegetation while still in full leaf. The use of the automated loggers helped to fully time-synchronize the data recording and avoid any bias associated with variation in time of data recording.

The repeated measurement of temperature and humidity at a fixed set of locations during 15 consecutive days can be characterized as pseudo-replication with two temporal dimensions. The first dimension is the variation in temperature within days and the second is the variation between days. The latter is of no interest to this study but repetition over 15 days was chosen to account for daily extremes in weather conditions and thereby ensure that the data was representative for the time period. We fitted linear mixed-effects models with serial correlation that allowed for nested random effects (Lindstrom & Bates, 1990) to examine the relationships between biophysical characteristics and microclimate in the parks, and to assess the influence of temporal variation in cooling efficiency of parks. The park biophysical characteristics included in the model were species category, canopy cover, crown depth, ground cover type, altitude, park size and shape. The principle of parsimony (Occam's razor) was applied for model reduction (Crawley, 2007). Parks and sample plots within each park were included as random factors in order to account for autocorrelation and pseudo-replication at each location.

The dataset was analyzed in two ways: First, hourly mean temperature across 15 days, with six repeated records of temperature every hour in the period from 10:00 to 15:59, were fitted using a first order autoregressive model (AR1) with correlation structure between hours across the day (Eq. (1)). Secondly, for each day the mean values of temperature in the morning (10:00–11:59), at noon (12:00–13:59) and in the afternoon (14:00–15:59) during the 15 days were analyzed to explore temporal variation in magnitude of thermal impacts of the parks. All analyses of microclimate data were carried out using the R language environment for statistical computing version 2.15.3 (R Development Core Team, 2013) and the extension package NLME (Pinheiro, Bates, DebRoy, Sarkar, & R Development Core Team, 2013).

The first order autoregressive model, emphasizing hourly mean temperature across 15 days, was formulated as:

$$y_{ijs} = \beta_0 + \beta_1 A_i + \beta_2 C_j + \beta_3 (S_l) + b_i + b_{ij} + k_s + \varepsilon_{ijs} \quad (1)$$

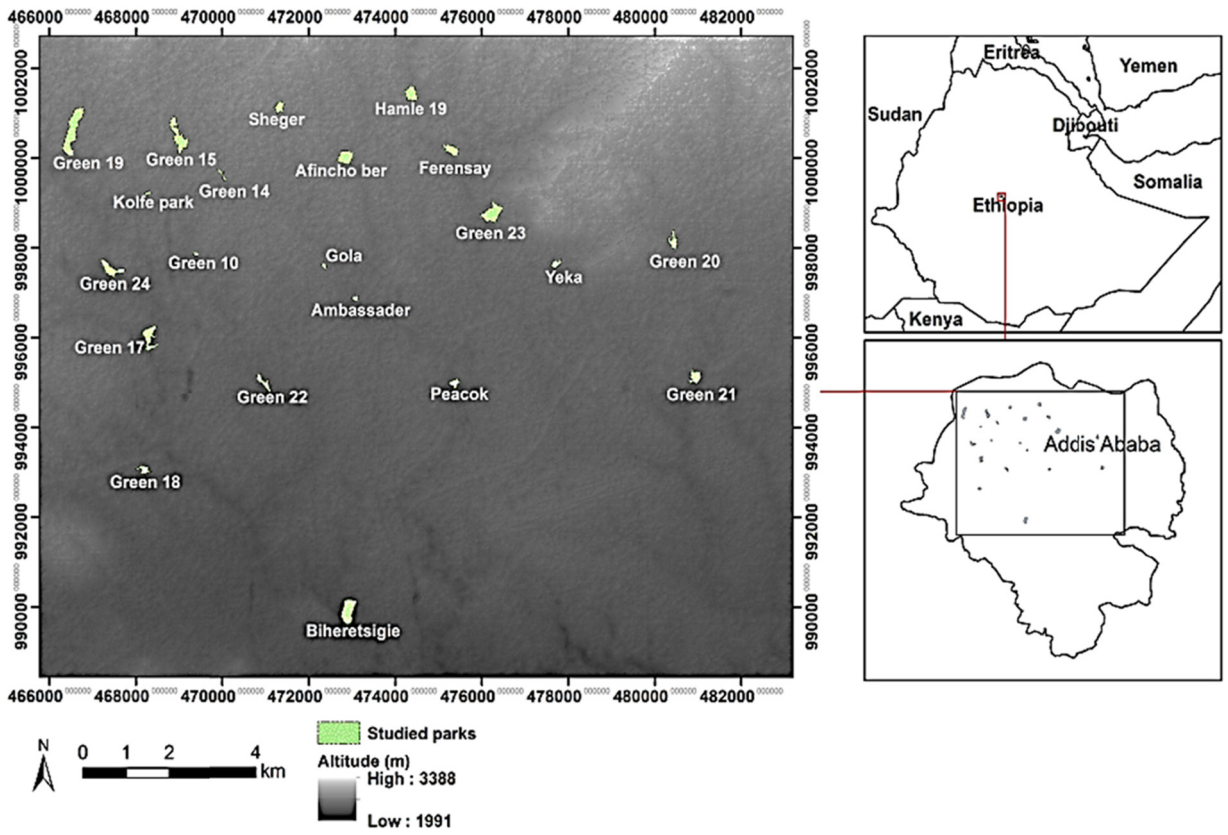

Fig. 1. Map of the study area showing individual parks overlaid on ASTER GDEM (30 m spatial grid). The boundary of the green areas was digitized from high resolution Google Earth™ imagery. The boundaries of the parks may not follow the actual administrative boundary. In cases where adjacent land cover is similar to the parks (e.g. Afincho ber), the demarcated area included both the park and adjacent green area. Parks included in the ground-based air temperature measurements are: Afincho ber, Biheretsigie, Ferensay, Gola, Hamle 19, Kolfe, Peacock, Sheger and Yeka.

where $i = 1, \ldots, 9$ (parks), $j = 1, \ldots, 60$ (locations within parks, i.e. plots), $l = 1, \ldots, 5$ (species types), $s = 1, \ldots, 6$ (hour of the day), $b_i \sim N(0, \psi_1)$, $b_{ij} \sim N(0, \psi_2)$, $k_s = pk_{s-1} + \eta_s$, $\varepsilon_{ijs} \sim N(0, \sigma^2 I)$, y_{ijs} is the temperature (°C) at the jth location repeated every hour (s), 10:00–15.59, and averaged across 15 successive days, β_0 is the general intercept; β_1, β_2 and β_3 are the parameters for the fixed effects; A and C are continuous fixed variables (altitude, m, and canopy cover, %); S is a fixed independent categorical variable with 5 levels representing the five species groups; b_i is the random effect for park with mean 0 and variance – covariance matrix ψ_1 for level-1 random effects, b_{ij} is the random effect for location (plot) nested within park with mean 0 and variance – covariance matrix ψ_2 for level-2 random effects, k_s is the serial autoregressive correlation structure of order 1 (AR1) for the repeated hourly measurements of temperature at the jth location, and ε_{ijs} is the within group error.

Eq. (2) shows the linear mixed-effect model with Gaussian correlation structure accounting for correlation between the 15 measurements dates (Eq. (2)). This model includes only one record of temperature per location for each of the 15 days, which is an average of temperatures during morning (10:00–11.59), noon (12:00–13:59) or the afternoon (14:00–15.59). In the morning data set, there is 730 observations (170 missing) and in the noon and afternoon data sets, there are 894 and 895 observations (with 6 and 5 missing values in the noon and afternoon, respectively). The model is formulated as:

$$y_{ijs} = \beta_0 + \beta_1 A_i + \beta_2 C_j + \beta_3 (S_l) + b_i + b_{ij} + \varepsilon_{ijs} \quad (2)$$

where $b_i \sim N(0, \psi_1)$, $b_{ij} \sim N(0, \psi_2)$, $\varepsilon_{ijs} \sim N(0, \sigma^2 I)$, and y_{ijs} is the temperature in the ith park and jth location (plot) on day $s = 1, \ldots, 15$. Otherwise, the notation is identical to that of Eq. (1).

2.2.2. Remotely sensed data

The purpose of using thermal remote sensing was to compare temperature within parks and in the surrounding non-park environment with the help of the dense, time-synchronized grid of data provided by the satellite sensor. Centers of Landsat pixels roughly correspond to centers of plots where ground-based microclimate measurement and park characterization were made. In addition to the thermal band that can be used to assess surface temperature, spatially detailed information on the characteristics of the land cover and intensity of tree vegetation can be derived from the Landsat images.

Land Surface Temperature (LST) was retrieved from a cloud-free sub-scene of Landsat ETM+, path 168 and row 54, acquired on 14 October 2010 and obtained from United States Geological Survey (USGS, 2012). The LST retrieval followed the procedures described in Weng et al. (2004), Artis and Carnahan (1982), and with calibration constants specified in NASA (2012). The dimension of the sub-scene is 42 km by 30 km (1400 by 1000 Landsat pixels of 30 m spatial resolution, the thermal band was re-sampled to 30 m resolution to match the reflective bands). A gap-filling tool in ENVI was used to fill the data gaps caused by the Scan Line Corrector (SLC) failure of Landsat 7 (NASA, 2012). An ETM+ image of 30 October 2010 was used for gap filling. The ETM+ images were terrain-corrected Level 1T products and georeferenced with precision better than 0.4 pixels (NASA, 2012).

Multiple buffer zones at 30 m intervals from the edge of parks to a maximum distance of 420 m were used to examine thermal differences between the parks and the surroundings (Fig. 2). Greenness levels of park vegetation and surrounding non-park environments were estimated using normalized difference

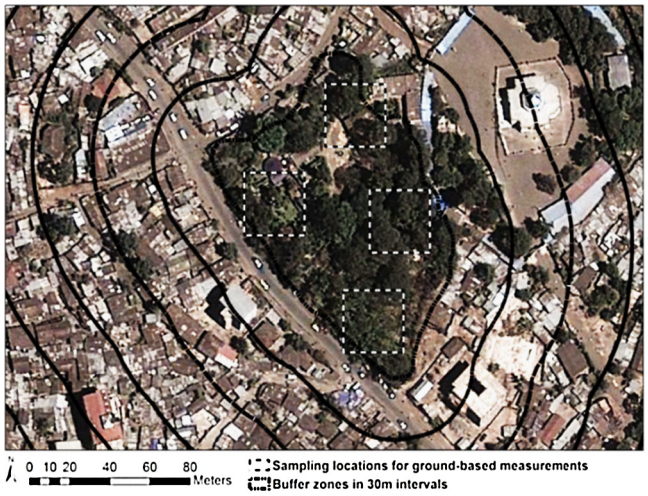

Fig. 2. Multiple ring buffer zones (30 m width) around Gola park and sample locations (shown on background image from Google Earth™).

vegetation index (NDVI). Moreover, the shape index (SI) of individual parks was calculated using the Patch Analyst tool developed by Rempel, Kaukinen, & Carr (2012).

At the first stage of the analysis variables describing the characteristics of parks, including park area (ha), shape index, edge density, perimeter-area ratio and NDVI were analyzed for their possible influence on surface temperature, both within parks and in the surrounding built-up environment. Park cooling intensity (PCI), which was considered a measure of the intensity of thermal contrast between park and surrounding non-park surfaces, was estimated using the model in Eq. (3). There is lack of consistency in the literature regarding the terminology used to describe the thermal contrast between park and non-park surroundings. Many studies use "Park Cool Island" (e.g. Spronken-Smith & Oke, 1999), while others use "Park Cooling Intensity" (e.g. Vanos et al., 2012) and "Park Cool Island intensity" (e.g. Lu, Li, Yang, Zhang, & Jin, 2012) to describe the same phenomenon of cooling impact of parks. PCI varied conspicuously with distance to parks (Fig. 3) but was also expected to depend on various features of the area surrounding each park, including the land cover type. As a basis for modeling the relationship between PCI and distance from park,

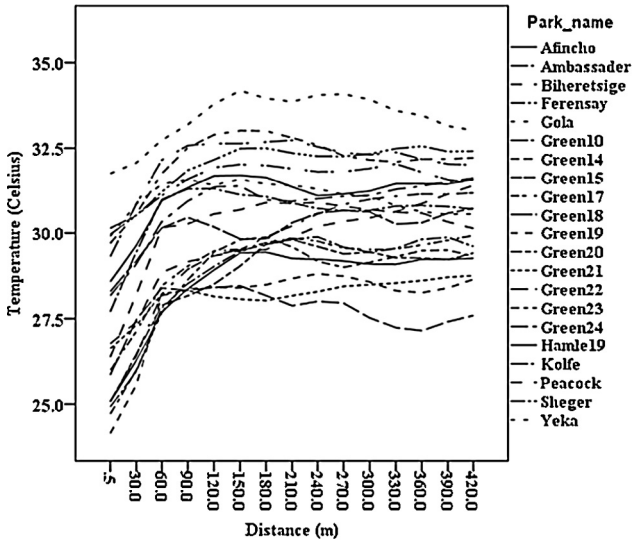

Fig. 3. Mean surface temperature versus distance from edge of parks. The mean temperature is calculated for each of the buffer rings at 30 m intervals.

a dataset describing average features of each of the multiple 30 m wide ring buffers around each park was prepared. Mean surface temperature of each of the multiple rings was calculated. Edge pixels consisting of mixture of park and non-park land covers were excluded from this calculation. Moreover, mean values of NDVI were calculated at park level and for each of the rings around parks. Ordinary Least Squares regression was used to evaluate how mean temperatures outside parks are influenced by park specific characteristics, distance from park and NDVI outside parks.

To obtain a distinct measure of the maximum distance within which the cooling effect of a park could still be detected (henceforth: park cooling distance, PCD, m), we applied a segmented non-linear model including a second-order polynomial and a horizontal upper level corresponding to maximum PCI. The PCD and the maximum PCI were assumed to depend on park area (ParkArea, ha), shape index (Park SI), mean altitude (Altitude, m), and longitude (Longitude, UTM easting in km) of the park and on average NDVI within each ring. Hence, the effect of park area on cooling distance was assumed to be non-linear and the model was specified as:

$$\mathrm{PCI}_{rp} = \begin{cases} a + b \times \mathrm{Dist}_{rp} + c \times \mathrm{Dist}_{rp}^2 + \varepsilon_{rp} & \text{if} \quad \mathrm{Dist}_{rp} < \mathrm{PCD}_p \\ \mathrm{PCI}_{\max} + \varepsilon_{rp} & \text{if} \quad \mathrm{Dist}_{rp} \geq \mathrm{PCD}_p \end{cases} \tag{3}$$

where $\mathrm{PCD}_p = \beta_0 + \beta_1 \times \mathrm{ParkArea}_p^{\delta} + \beta_2 \times \mathrm{Park\ SI}_p + \beta_3 \times \mathrm{Altitude}_p + \beta_4 \times \mathrm{Longitude}_p$, $\mathrm{PCI}_{\max} = \gamma_p + \gamma_0 \times \mathrm{NDVI}_{rp}$, $a = \mathrm{PCI}_{\max} + c \times \mathrm{PCD}_p^2$ and $b = -2 \times c \times \mathrm{PCD}_p$and c, $\beta_0 \ldots \beta_4$, δ, and γ_0 and γ_p are parameters to be estimated, $p = 1, \ldots, 21$ are the parks and $r = 1, \ldots, 14$ are the ring buffer zones. The residuals, ε_{rp}, were assumed to be normally distributed with variance inversely proportional to ring buffer area. For each park γ_p expresses the general difference between the temperature of the park and its wider surroundings. Model parameters were estimated using weighted non-linear regression (weight: ring area) and the NLIN procedure of the SAS software package (v. 9.2).

3. Results

3.1. Variation in cooling effect of parks

A significant negative relationship was observed between temperature and canopy cover ($P < 0.001$). The temperature dropped by 0.02 °C for every percent increase in tree canopy cover (Table 1a). Among the species groups, *Eucalyptus* showed the highest temperature reduction followed by *Olea*, while the *Grevillea* and *Cupressus* groups exhibited the lowest cooling effect. The cooling effect of *Eucalyptus* was significantly higher ($P < 0.05$) than that of any other species (Table 1a and b). *Olea* also showed significantly higher cooling effect than *Cupressus* ($P < 0.05$). In the comparison made on the basis of the data where temperatures were aggregated in the morning, noon and afternoon and where the effect of individual days were accounted for in the model, it was observed that *Eucalyptus* had a significantly higher cooling effect in the morning and at noon than *Cupressus, Grevillea* and *Olea* ($P < 0.05$). In the afternoon *Eucalyptus* had a significantly higher effect than *Cupressus, Grevillea* and *Acacia.* (Table 1c). Fig. 4 shows the patterns of mean temperature in the morning (Fig. 4A) and afternoon (Fig. 4B) across the 15 days for each park and species. Although *Eucalyptus* is not found in all parks its distinct cooling effect is clearly indicated.

Altitude was found to be significantly and negatively related to temperature in all models evaluated in this study. This relationship is also clearly seen in Fig. 4 where the general temperature level decreases with increasing mean altitude of the parks. Other biophysical factors including type of ground cover, ground moisture, canopy depth, park size and shape showed no significant

Table 1
Parameter estimates and significance tests of linear mixed-effect models describing mean hourly temperature (°C) as a function of tree species category, canopy cover (%) and altitude (m): (a) Mixed effects model for mean hourly temperature 10:00–15:59 averaged across 15 days and with temporal within-day autocorrelation accounted for; (b) table of contrasts for the model in (a) showing pairwise comparison of species; and (c) mixed-effects model for mean temperature for three time intervals: late morning (10:00–11:59), noon (12:00–13.59) and early afternoon (14:00–15.59).

(a)

Variable	Parameters	Std. error	*P*-value
(Intercept)	53.538	7.825	0.000
Cupressus	1.214	0.294	0.000
Accacia	0.961	0.431	0.031
Grevillea	1.194	0.337	0.001
Olea	0.737	0.329	0.030
Canopy cover	−0.017	0.004	0.000
Altitude	−0.012	0.003	0.000

(b)

Species	Reference species				
	Eucalyptus	*Accacia*	*Cupressus*	*Grevillea*	*Olea*
Eucalyptus		0.0307	0.0001	0.0009	0.0301
Accacia			0.471	0.5912	0.5579
Cupressus				0.9499	0.0445
Grevillea					0.2084
Olea					

(C)

Variables	10:00–11:59			12:00–13:59			14:00–15:59		
	Value	Std. error	*P*-value	Value	Std. error	*P*-value	Value	Std. error	*P*-value
Intercept	46.487	9.889	0.000	54.431	6.728	0.000	57.234	7.789	0.000
Eucalyptus	0.000			0.000			0.000		
Acacia	0.795	0.476	0.102	0.838	0.450	0.069	1.062	0.379	0.007
Cupressus	1.359	0.325	0.000	1.140	0.307	0.001	1.097	0.259	0.000
Grevillea	1.226	0.369	0.002	1.095	0.352	0.003	1.240	0.295	0.000
Olea	1.252	0.362	0.001	0.722	0.344	0.042	0.565	0.289	0.057
Canopy cover	−0.023	0.005	0.000	−0.024	0.005	0.000	−0.015	0.004	0.000
Altitude	−0.009	0.004	0.027	−0.012	0.003	0.000	−0.014	0.003	0.000

relationship with air temperature. The humidity variation among species and parks was not statistically significant.

3.2. Park cooling intensity and cooling distance

The mean surface temperature of 30 m wide buffer zones, from the edge of each park to a maximum distance of 420 m, was significantly influenced by park size, park NDVI, NDVI within each individual ring, shape index of the park and distance from park. A summary of the linear regression model is shown in Table 2(A, left) and indicates that temperature outside the park is negatively related to park size and NDVI values within and outside the park. Similarly, it appears that mean temperature outside the park is significantly and negatively related to park shape index (SI). Finally, a significant positive relationship was detected between distance from park and mean temperature outside park (Table 2A).

The park cooling intensity (PCI) was positively related to park size and NDVI within parks, implying that a higher thermal

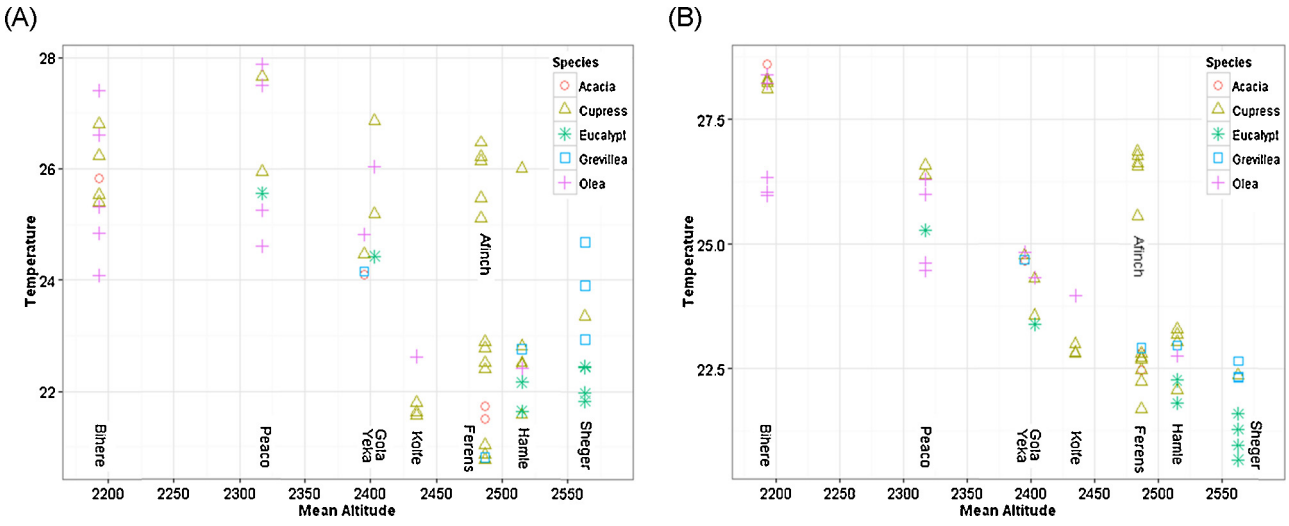

Fig. 4. Mean temperature of locations within parks sorted by altitude: late morning hours (10:00–11:59) (A) and early afternoon hours (14:00–15.59) (B).

Table 2
Multiple linear regressions showing relationships between (A) mean temperature outside park (°C) (n = 358, DF 352, Adj. R^2 = 0.825), (B) Park cooling intensity (PCI, °C) (n = 358, df = 352, Adj. R^2 = 0.56) and independent variables describing park characteristics, NDVI of 30 m wide ring buffer zones and distance from park.

A: Mean temperature outside park				B: Park cooling intensity			
Variables	Value	Std. error	P-value	Variables	Value	Std. error	P-value
(Intercept)	36.31	0.446	0.000	(Intercept)	1.115	0.5925	<0.001
Park area (ha)	−0.100	0.011	0.000	Park Area (ha)	0.110	0.015	<0.001
Park NDVI	−2.564	1.053	<0.02	Park NDVI	10.740	1.399	<0.001
Park SI[a]	−0.477	0.194	<0.02	Park SI[a]	−0.869	0.251	<0.01
Ring NDVI	−15.740	0.749	0.000	Ring NDVI	−10.410	0.994	0.000
Distance (m)	0.002	0.0005	<0.01	Distance (m)	0.004	0.0006	<0.01

[a] Shape index.

contrast is observed as the area or intensity of greenness of parks increase (Table 2B). This finding is also supported by the ground measurement results where low mean temperature of parks was associated with high canopy cover intensity. On the other hand, PCI was negatively related to NDVI outside parks (Table 2B). Obviously, in situations where the landscape surrounding a park consists of some sort of green space, the thermal properties of the surroundings will be similar to the park; hence less thermal contrast between park and non-park will be observed with increasing NDVI outside park. On average, a cooling intensity of 3.93 °C (ranging from 0.11 to 6.72 °C) was observed.

The park cooling distance (PCD) was significantly and positively related to size of parks, shape index (SI) and altitude (Table 2B). In addition it turned out that there was a significant effect of longitude. The model offers a very good fit (R^2 = 0.95) and as expected the effect of park area is positive (δ and β_1 are both negative) (Table 3). A maximum cooling distance of 224 m was estimated.

4. Discussion

Our study which involved coupled air temperature measurements in multiple parks and thermal remote sensing indicated that the cooling effect of parks on the surrounding landscape depended considerably on tree species and physical characteristics of the park, including canopy intensity, size and shape of park, altitude, time of the day, and characteristics of surrounding non-park areas.

The higher cooling effect of *Eucalyptus* species compared to other species groups is an interesting observation. A study of similar nature undertaken in Israel by Shashua-Bar et al. (2009) showed that *Ficus* and *Tipuana tipu* trees were more effective in cooling compared to Date Palm trees (*Phoenix*). Lin and Lin (2010) also compared cooling effects of 12 tree species in a park in Taipei city, Taiwan and reported *Ulmus parvifolia* to be most effective in cooling. Our findings which showed relatively less cooling for *Grevillea* and *Cupressus* species compared to *Eucalyptus* may seem to be contrary to a study by Leuzinger, Vogt, and Korner (2010) who concluded that trees with larger leaves generally tend to have higher crown temperature. On the other hand, Oke (1988) showed conifers to absorb more radiation which may imply higher temperature under conifers compared to broadleaved species. Differences in canopy structure, thermal and optical properties of the tree species may possibly determine the cooling efficiency.

The temporal variation in cooling efficiency of the species compared in this study could be related to differences in rate of transpiration of plants at different times of day (Goyal, 2004; Tuzet, Perrier, & Leuning, 2003). Plants may minimize the amount of moisture released through evapotranspiration, thereby reducing their cooling efficiency. Similar temporal variation in cooling was reported in other studies such as Lu et al. (2012) and Oliveira et al. (2011). Lu et al. (2012) argued that the low intensity of PCI shown in their study could be related to the photosynthesis midday depression (PMD) causing low evaporative cooling at 13:00. Plants in the 21 parks may tend to close their stomata during midday as a result of intense solar radiation, leading to less photosynthesis and reduced cooling effect of evapotranspiration.

The results indicate that high intensity of tree canopy cover (and NDVI in case of remotely sensed data) led to significantly higher cooling effect at all times of the days. This is a clear indication that the density of vegetation in parks plays a vital role in enhancing the cooling effect on daytime air temperature. An experimental study by Shashua-Bar et al. (2009) in hot environments obtained similar results where the shading effect of trees cooled the air significantly more than the same amount of shade provided by other means. The findings from our thermal remote sensing study are also in agreement with a number of urban climate studies that involved similar data types (Amiri, Weng, Alimohammadi, & Alavipanah, 2009; Chen, Zhao, Li, & Yin, 2006; Hung et al., 2006). The positive relationship between park size and PCI observed in this study is in agreement with studies such as Lu et al. (2012) and Cao, Onishi, Chen, and Imura (2010). Cao et al. (2010) reported a maximum daytime surface temperature difference of 5.8 °C between parks and the surrounding non-park environment.

The results also showed that parks with higher shape index (SI) had greater cooling distance, but less cooling intensity,

Table 3
Parameter estimates for the segmented park cooling model in Eq. (3). N = 315, R^2 = 0.95, F = 187 (Pr > F < 0.0001).

Parameter	Role of parameter	Estimate	Std. error	Approximate 95% confidence limits	
c	Dist^2 coeff	−71.5838	12.7101	−96.6010	−46.5666
β_0	PCD intercept	−2.3219	0.5362	−3.3774	−1.2664
β_1	ParkArea coeff	−0.1848	0.0506	−0.2843	−0.0853
β_2	ParkSI coeff.	0.0749	0.0156	0.0442	0.1056
β_3	Altitude coeff.	0.00026	0.00005	0.00016	0.00036
β_4	Longitude coeff.	0.00377	0.00107	0.00167	0.00588
δ	ParkArea power	−0.8443	0.4820	−1.7930	0.1044
γ_0	NDVI coeff.	−9.5048	0.8271	−11.1327	−7.8769
γ_p range	PCI_{max} intercept[a]				
Min. γ_p		3.3904	0.1675	3.0606	3.7201
Max. γ_p		8.6909	0.2181	8.2615	9.1203

[a] Park specific value.

implying that compact parks with shape closer to that of a circle have higher thermal contrast with their immediate surroundings than elongated parks. On the other hand, parks that have more irregular shape tended to have higher park cooling distance (PCD), indicating that the larger area of the zone where irregular parks are in contact with the surrounding non-park landscape may increase the distance within which parks influence the thermal environment. Increasing irregularity of shape of parks, therefore, seems to have contrasting effects on cooling intensity and cooling distance. Variation in intensity of PCI may also be influenced by the specific characteristics of the surrounding environment and the time of the day. Anthropogenic waste heat that is injected into the surrounding environment from intense traffic could increase the contrast between surface temperature of the parks and that of the surroundings. The variation in thermal properties of different types of built surfaces, such as asphalt roads and building roofs could also contribute to surface temperature variation in the surrounding non-park environment (Gartland, 2008).

5. Conclusion and perspectives

In this study we used ground-based air temperature measurements and satellite thermal remote sensing to evaluate cooling effects of parks and examined the relationships between park characteristics and temperature. We conclude that, within the same city, the cooling efficiency of urban tree vegetation varied with park specific characteristics including species composition, canopy intensity, size and shape of the parks. Moreover, intra-urban variation in altitude also played a significant role in determining thermal variation among parks. Irregular and elongated parks were shown to have lower PCI and higher PCD compared to regularly shaped, compact parks. Both PCI and PCD were shown to increase with park size.

This study provides insight regarding the importance of evaluating the effectiveness of urban green spaces in mitigating the heat island effect. Understanding differences in cooling effects among parks may help urban planners and greening designers to make appropriate decisions regarding species choice, and size and shape of green spaces. The main recommendations based on this study in terms of maximizing cooling effects of parks are to increase tree vegetation canopy cover, optimize park size and shape, and prioritize the choice of species for greening. Our results suggest that *Eucalyptus, Olea and to some extent Acacia* are more effective in cooling the urban environment than *Cupressus and Grevillea*. However, apart from cooling there are a number of other environmental and social services that are provided by urban green spaces and which need to be considered carefully before deciding about the choice of species.

In many instances, urban greening seems to emphasize the esthetic values of parks and other green spaces and tends to overlook the local climatic influence of vegetation. Hence, urban greening efforts in Addis Ababa and areas with similar environments may need to integrate and optimize the multiple environmental and social values of green spaces.

Since only 21 green spaces were considered in the remote sensing component of the study and microclimate data were monitored within only 9 of the parks and for only 15 days, the study may not fully represent the diurnal, seasonal and annual variations of the cooling effect of parks. Therefore, further studies need to be undertaken for better understanding the cooling efficiency and for making specific recommendations for city planners. Studies that involve a large number of sample parks from multiple cities and comparison of larger numbers of tree species may provide more generalizable results. Seasonal variation in foliage density and evaporative cooling may need to be explored. Observational studies may also need to be combined with a controlled experimental set-up. Evaluation of cooling effects of non-park green spaces such as street trees, private gardens and green roofs could also help understanding how green infrastructure can be integrated in urban environments to efficiently mitigate heat island effects and to improve the quality of life in cities. Estimation of optimal park shape and size that maximizes the combined PCI and PCD and also includes benefits other than cooling is an important perspective.

References

Akbari, H., Pomerantz, M., & Taha, H. (2001). Cool surfaces and shade trees to reduce energy use and improve air quality in urban areas. *Solar Energy*, *70*, 295–310.

Amiri, R., Weng, Q. H., Alimohammadi, A., & Alavipanah, S. K. (2009). Spatial-temporal dynamics of land surface temperature in relation to fractional vegetation cover and land use/cover in the Tabriz urban area, Iran. *Remote Sensing of Environment*, *113*, 2606–2617.

Arnfield, A. J. (2003). Two decades of urban climate research: A review of turbulence, exchanges of energy and water, and the urban heat island. *International Journal of Climatology*, *23*, 1–26.

Bowler, D. E., Buyung-Ali, L., Knight, T. M., & Pullin, A. S. (2010). Urban greening to cool towns and cities: A systematic review of the empirical evidence. *Landscape and Urban Planning*, *97*, 147–155.

Cao, X., Onishi, A., Chen, J., & Imura, H. (2010). Quantifying the cool island intensity of urban parks using ASTER and IKONOS data. *Landscape and Urban Planning*, *96*, 224–231.

Central Statistics Agency (CSA). (2012). *Population 2012*. Available online at, http://www.csa.gov.et/index.php/2013-02-20-13-43-35/national-statistics-abstract/141-population Accessed 22.10.13

Chen, X. L., Zhao, H. M., Li, P. X., & Yin, Z. Y. (2006). Remote sensing image-based analysis of the relationship between urban heat island and land use/cover changes. *Remote Sensing of Environment*, *104*, 133–146.

Chen, X. Z., Su, Y. X., Li, D., Huang, G. Q., Chen, W. Q., & Chen, S. S. (2012). Study on the cooling effects of urban parks on surrounding environments using Landsat TM data: A case study in Guangzhou, southern China. *International Journal of Remote Sensing*, *33*, 5889–5914.

Conway, D., Mould, C., & Bewket, W. (2004). Over one century of rainfall and temperature observations in Addis Ababa, Ethiopia. *International Journal of Climatology*, *24*, 77–91.

Corburn, J. (2009). Cities, climate change and urban heat island mitigation: Localising global environmental science. *Urban Studies*, *46*, 413–427.

Cornelis, J., & Hermy, M. (2004). Biodiversity relationships in urban and suburban parks in Flanders. *Landscape and Urban Planning*, *69*, 385–401.

Dallimer, M., Irvine, K. N., Skinner, A. M. J., Davies, Z. G., Rouquette, J. R., Maltby, L. L., et al. (2012). Biodiversity and the feel-good factor: Understanding associations between self-reported human well-being and species richness. *Bioscience*, *62*, 47–55.

Dallimer, M., Rouquette, J. R., Skinner, A. M. J., Armsworth, P. R., Maltby, L. M., Warren, P. H., et al. (2012). Contrasting patterns in species richness of birds, butterflies and plants along riparian corridors in an urban landscape. *Diversity and Distributions*, *18*, 742–753.

Debruin, H. A. R., & Jacobs, C. M. J. (1993). Impact of CO_2 enrichment on the regional evapotranspiration of agroecosystems, a theoretical and numerical modeling study. *Vegetatio*, *104*, 307–318.

Dimoudi, A., & Nikolopoulou, M. (2003). Vegetation in the urban environment: Microclimatic analysis and benefits. *Energy and Buildings*, *35*, 69–76.

Escobedo, F., Varela, S., Zhao, M., Wagner, J. E., & Zipperer, W. (2010). Analyzing the efficacy of subtropical urban forests in offsetting carbon emissions from cities. *Environmental Science & Policy*, *14*, 1219.

Gartland, L. (2008). *Heat island: Understanding and mitigating heat in urban areas*. London/Sterling, VA: Earthscan.

Georgi, N. J., & Zafiriadis, K. (2006). The impact of park trees on microclimate in urban areas. *Urban Ecosystems*, *9*, 195–209.

Goyal, R. K. (2004). Sensitivity of evapotranspiration to global warming: A case study of arid zone of Rajasthan (India). *Agricultural Water Management*, *69*, 1–11.

Hajat, S., Kovats, R. S., & Lachowycz, K. (2007). Heat-related and cold-related deaths in England and Wales: Who is at risk? *Occupational and Environmental Medicine*, *64*, 93–100.

Hung, T., Uchihama, D., Ochi, S., & Yasuoka, Y. (2006). Assessment with satellite data of the urban heat island effects in Asian mega cities. *International Journal of Applied Earth Observation and Geoinformation*, *8*, 34–48.

Jacob, D. J., & Winner, D. A. (2009). Effect of climate change on air quality. *Atmospheric Environment*, *43*, 51–63.

Jana, B. K., Biswas, S., Majumder, M., Roy, P., & Mazumdar, A. (2010). Accumulation of carbon stock through plantation in urban area. In B. K. Jana, & M. Majumder (Eds.), *Impact of climate change on natural resource management.* (pp. 281–294). London, New York: Springer Science + Business Media.

Jonsson, P. (2004). Vegetation as an urban climate control in the subtropical city of Gaborone, Botswana. *International Journal of Climatology*, *24*, 1307–1322.

Leuzinger, S., Vogt, R., & Korner, C. (2010). Tree surface temperature in an urban environment. *Agricultural and Forest Meteorology*, *150*, 56–62.

Lin, B. S., & Lin, Y. J. (2010). Cooling effect of shade trees with different characteristics in a subtropical urban park. *Hortscience*, *45*, 83–86.

Lindstrom, M. J., & Bates, D. M. (1990). Nonlinear mixed effects models for repeated measures data. *Biometrics*, *46*, 673–687.
Lu, J., Li, C.-D., Yang, Y.-C., Zhang, X.-H., & Jin, M. (2012). Quantitative evaluation of urban park cool island factors in mountain city. *Journal of Central South University*, *19*, 1657–1662.
McKibben, B. (2007). Climate change 2007: The physical science basis: Summary for policymakers. *New York Review of Books*, *54*, 44–45.
NASA. (2012). *Landsat 7 science data users handbook*. (Online).
Oke, T. R. (1988). *Boundary layer climates* (2nd ed.). London and New York: Methuen & Co., Ltd. and Methuen, Inc.
Oliveira, S., Andrade, H., & Vaz, T. (2011). The cooling effect of green spaces as a contribution to the mitigation of urban heat: A case study in Lisbon. *Building and Environment*, *46*, 2186–2194.
Patz, J. A., Campbell-Lendrum, D., Holloway, T., & Foley, J. A. (2005). Impact of regional climate change on human health. *Nature*, *438*, 310–317.
Pearlmutter, D., Bitan, A., & Berliner, P. (1999). Microclimatic analysis of "compact" urban canyons in an arid zone. *Atmospheric Environment*, *33*, 4143–4150.
Pinheiro, J., Bates, D., DebRoy, S., Sarkar, D., & R Development Core Team. (2013). NLME: Linear and nonlinear mixed effects models. In *R package version 3.1-109*.
Pugnaire, I. F., & Valladares, F. (Eds.). (2007). *Functional plant ecology*. Boca Raton, FL: CRC Press, Taylor & Francis Group.
Quattrochi, D. A., & Luvall, J. C. (1999). Thermal infrared remote sensing for analysis of landscape ecological processes: Methods and applications. *Landscape Ecology*, *14*, 577–598.
R Development Core Team. (2013). *A language and environment for statistical computing*. Vienna, Austria: R Foundation for Statistical Computing. http://www.R-project.org
Rempel, R. S., Kaukinen, D., & Carr, A. P. (2012). Patch analyst and patch grid. In *C.f.N.F.E.R. Ontario Ministry of Natural Resource*. Ontario: Thunder Bay (Ed.).
Ren, Y., Wei, X., Wei, X., Pan, J., Xie, P., Song, X., et al. (2011). Relationship between vegetation carbon storage and urbanization: A case study of Xiamen, China. *Forest Ecology and Management*, *261*, 1214–1223.
Schwarz, N., Schlink, U., Franck, U., & Grossmann, K. (2012). Relationship of land surface and air temperatures and its implications for quantifying urban heat island indicators – An application for the city of Leipzig (Germany). *Ecological Indicators*, *18*, 693–704.
Shashua-Bar, L., Pearlmutter, D., & Erell, E. (2009). The cooling efficiency of urban landscape strategies in a hot dry climate. *Landscape and Urban Planning*, *92*, 179–186.
Shen, T., Chow, D. H. C., & Darkwa, J. (2013). Simulating the influence of microclimatic design on mitigating the Urban Heat Island effect in the Hangzhou Metropolitan Area of China. *International Journal of Low-Carbon Technologies*, http://dx.doi.org/10.1093/ijlct/ctt050
Smith, C., & Levermore, G. (2008). Designing urban spaces and buildings to improve sustainability and quality of life in a warmer world. *Energy Policy*, *36*, 4558–4562.
Spronken-Smith, R. A., & Oke, T. R. (1999). Scale modelling of nocturnal cooling in urban parks. *Boundary-Layer Meteorology*, *93*, 287–312.
Susca, T., Gaffin, S. R., & Dell'Osso, G. R. (2011). Positive effects of vegetation: Urban heat island and green roofs. *Environmental Pollution*, *159*, 2119–2126.
Taha, H. (1997). Urban climates and heat islands: Albedo, evapotranspiration, and anthropogenic heat. *Energy and Buildings*, *25*, 99–103.
Tallis, M., Taylor, G., Sinnett, D., & Freer-Smith, P. (2011). Estimating the removal of atmospheric particulate pollution by the urban tree canopy of London, under current and future environments. *Landscape and Urban Planning*, *103*, 129–138.
Tan, J. G., Zheng, Y. F., Tang, X., Guo, C. Y., Li, L. P., Song, G. X., et al. (2010). The urban heat island and its impact on heat waves and human health in Shanghai. *International Journal of Biometeorology*, *54*, 75–84.
Tremeac, B., Bousquet, P., de Munck, C., Pigeon, G., Masson, V., Marchadier, C., et al. (2012). Influence of air conditioning management on heat island in Paris air street temperatures. *Applied Energy*, *95*, 102–110.
Tuzet, A., Perrier, A., & Leuning, R. (2003). A coupled model of stomatal conductance, photosynthesis and transpiration. *Plant Cell and Environment*, *26*, 1097–1116.
UN-HABITAT. (2008). *State of the world's cities 2010/2011: Bridging the urban divide*. Earthscan, London: United Nations Human Settlements Programme (UN-HABITAT).
United States Geological Survey (USGS). (2012). Landsat data archive. In *Global visualization viewer (GLOVIS)*.
Voogt, J. A., & Oke, T. R. (1998). Effects of urban surface geometry on remotely-sensed surface temperature. *International Journal of Remote Sensing*, *19*, 895–920.
Voogt, J. A., & Oke, T. R. (2003). Thermal remote sensing of urban climates. *Remote Sensing of Environment*, *86*, 370–384.
Weaver, C. P., Liang, X. Z., Zhu, J., Adams, P. J., Amar, P., Avise, J., et al. (2009). A preliminary synthesis of modeled climate change impacts on US regional ozone concentrations. *Bulletin of the American Meteorological Society*, *90*, 1843–1863.
Yin, S., Shen, Z., Zhou, P., Zou, X., Che, S., & Wang, W. (2011). Quantifying air pollution attenuation within urban parks: An experimental approach in Shanghai, China. *Environmental Pollution*, *159*, 2155–2163.